Performance analysis of SnO_x thin-film transistor including gas pulsing effects: Experimental and numerical modeling study

F. Djeffal[1,*], H. Ferhati[1,2], L.B. Drissi[3] and N. Martin[4,**]

[1] LEA, University of Batna 2, Batna 05000, Algeria
[2] ISTA, University of Larbi Ben M'hidi, Oum El Bouaghi, Algeria
[3]LPHE-MS, Faculty of Science, Mohammed V University in Rabat,Rabat, Morocco
[4] SUPMICROTECH, CNRS, Institut FEMTO-ST, BESANCON Cedex, France
*E-mails:faycal.djeffal@univ-batna2.dz; ** Nicolas.martin@femto-st.fr

Abstract

This work investigates the influence of the Reactive Gas Pulsing Process (RGPP) on the structural, electrical, and device-level performance of SnO_x thin-film transistors (TFTs). Both n-type and p-type SnO_x films were fabricated using DC sputtering under varied oxygen pulsing durations (8 s, 12 s, and 20 s). Structural and morphological properties were analyzed using X-ray diffraction (XRD) and Scanning Electron Microscopy (SEM), while Hall Effect measurements were employed to extract electrical parameters including resistivity, carrier mobility, and concentration. The RGPP enabled modulation of the oxygen stoichiometry and consequently the conductivity type and electrical behavior of the films. These experimentally extracted parameters were used as input data for numerical TCAD simulations of SnO_x-based TFTs using Silvaco simulator tool. The simulations confirmed that optimal RGPP conditions (12 s) lead to enhanced electrical performance, including a high ON current and low OFF current, yielding an ON/OFF current ratio of ~176 dB. Band alignment diagrams further support the observed electronic conduction behavior as a function of pulse duration. These findings highlight the potential of RGPP for tuning SnO_x properties, paving the way for its application in flexible and cost-effective electronic systems.

Keywords: SnO_x; TFT; sputtering; reactive gas; modeling; RGPP.

1. Introduction

During the last few years, flexible electronics have triggered a great deal of attention due to the growing demand for natural contact between humans and technological devices [1-5]. Thin-film flexible technology, combined with wireless devices open up new pathways for caring out real-time, continuous, and effective biometric signals [5]. Thin-film transistors (TFTs) are considered as key component in flexible electronics, which can be used as sensors or incorporated in integrated circuits for signal detection applications [4-5]. This is mainly due to their fascinating characteristics including high carrier mobility, tunable carrier concentration and conductivity, ability for low thermal budget, less processing complexity, and cost-effective elaboration [5].

Recently, amorphous metal oxide semiconductors such as IGZO, ZnO, ZnSnO, CuO_2 and SnO_2 are widely used as active films for TFT devices, which are widely exploited in various applications including storage memory, logic circuits and wearable electronics. This is mainly due to their flexibility, high transparency, good electron mobility, and improved surface properties [4-8]. Particularly, indium-based metal oxide materials like IGZO and IZO have been extensively used for TFTs, offering a high carrier mobility that exceeds 10 cm^2/Vs [7]. In addition to widely studied amorphous oxide semiconductors, recent studies have highlighted other promising materials, including Ga_2O_3, Ga_2O_3/TeO_2 bilayers, In-doped Ga_2O_3, porous SnO_2 structures, and ZnO/SnO_2 heterojunctions. These materials exhibit favorable optoelectronic and structural properties, making them attractive candidates for next-generation thin-film transistors and sensing applications [8], [9]. Incorporating such diverse materials expands the design space for optimizing performance and process compatibility in amorphous oxide-based devices. Despite these advantages, the demand for alternative Critical Raw Materials (CRM)-free based-devices prevent the deployment of IGZO-based TFT devices in various electronic applications. For this reason, researchers have turned out towards exploring

alternative metal oxide materials as active layers like SnO_2 and ZnO [6-8]. However, TFTs based on CRM-free metal oxides face several challenges involving the low derived current capability, poor resistive behavior and degraded switching characteristics. These issues are mainly related to the low carrier mobility and the high resistivity associated with CRM-free metal oxide thin-films, thus limiting the performance of the devices. On the other hand, electronic circuits based on TFT compounds are commonly composed of only n-type devices, where the developed p-type thin-film transistors still exhibit degraded electrical performances [8-11]. This is mainly correlated with the scarcity of appropriate p-type CRM-free metal oxides, reduced carrier mobility, degraded structural characteristics and processing complexity. Particularly, various p-type metal oxide semiconducting materials such as CuO, NiO, doped-CuO, CuSCN and SnO compounds have been widely investigated for the development of p-type conductivity TFT devices [12-14]. However, the recorded electrical performances of these p-type-based TFT devices are still far from the performance level of their counterpart based on n-type metal oxides. Consequently, it seems crucial to develop high-performance n-type and p-type TFT devices based on CRM-free materials. Following this direction, research efforts have been paid to SnO as alternative CRM-free material for enhancing the electrical performances of TFT devices. This is mainly due to its low elaboration cost, good electrical properties, tunable n-type and p-type conductivity [15-17]. However, the recorded electrical performances are still far from the expectation and new strategies are required to develop high-performance TFT devices for advanced electronic systems. Therefore, the development of new efficient CRM-free TFT structures is becoming a research trend to overcome these limitations and promote new opportunities for the development of the complementary integrated circuit based on p-type and n-type and oxide TFTs.

The growing demand for high-performance, low-cost, and flexible electronic devices has intensified research into oxide semiconductor-based thin-film transistors (TFTs), particularly

those utilizing environmentally friendly materials such as tin oxide (SnO_x) [15-18]. However, conventional deposition techniques often lack the precision required to control the electrical conductivity type and stoichiometry of SnO_x, both of which are critical for optimizing device performance. This study is motivated by the need for more adaptable and controllable fabrication strategies that enable precise tailoring of material properties. In this regard, we introduce the Reactive Gas Pulsing Process (RGPP) during DC sputtering as an innovative approach to engineer the structural and electrical characteristics of both n-type and p-type SnO_x thin films. Unlike traditional methods, RGPP allows real-time modulation of oxygen partial pressure during deposition, offering fine control over the resulting conductivity type. To the best of our knowledge, this is the first comprehensive investigation that combines experimental techniques and TCAD-based simulation to evaluate the effects of RGPP on SnO_x -based TFTs. Our integrated methodology provides a detailed understanding of how deposition parameters influence the physical and electrical behavior of the material and devices, confirming the potential of RGPP for the realization of next-generation flexible oxide electronics. Recent studies [17–19] have shown that RGPP is capable of modulating not only the oxygen content but also the conductivity type of various metal oxide semiconductors. This promising capability can be leveraged to develop both p-type and n-type SnO_x -based TFTs. In this work, we explore the impact of controlled oxygen pulsing on the structural, surface morphological, and electrical properties of SnO_x thin films. SnO_x layers were deposited via DC sputtering using three distinct oxygen pulsing durations (8 s, 12 s, and 20 s). Structural and surface characterizations were carried out using X-ray diffraction (XRD) and scanning electron microscopy (SEM), while Hall Effect measurements were employed to extract key electrical parameters including resistivity, carrier mobility, and carrier concentration. The elaborated SnO_x thin films were subsequently integrated as active layers in TFT devices, and their electrical performances were evaluated using rigorous TCAD simulations. The results demonstrate that the RGPP method enables

precise tuning of the film properties, significantly enhancing device performance. This confirms the suitability of oxygen-controlled pulsing as a reliable and scalable approach for fabricating high-performance TFTs, particularly for applications in flexible and low-power electronic systems.

2. Growth and analysis of SnO_x TFT

2.1. SnO_x thin-film deposition and characterization

SnO_x thin-films were deposited on glass substrates via combined DC sputtering and RGPP technique. This elaboration method is chosen for its ability for depositing high quality films with improved homogeneity, tunable film thickness and oxygen concentration. The sputtering process was carried out in 40 L vacuum chamber. The pulsing time associated with RGPP process is fixed at 8 s, 12 s and 20 s to elaborate SnO_x thin-films with n-type and p-type conductivity [17] and [19-21]. In this context, Fig.1 (a) shows a schematic description of RGPP method representing oxygen mass flow rate versus deposition time. We can notice that a pulsing signal with respect to the deposition time was used. The RGPP ON and OFF times (t_{ON} and t_{OFF}) are illustrated in the figure, corresponding to the oxygen pulsing of the rectangular signal under consideration. Here, P represents the pulsing period, and α denotes the duty cycle, defined as $\alpha = t_{ON}/P$. During the deposition process, P was maintained at 20 seconds, while α was adjusted between 0% and 100% of P, allowing a gradual change in α. The maximum and minimum oxygen flow rates were set at 2.4 sccm and 0 sccm during the t_{ON} and t_{OFF} times, respectively. To maintain consistent film growth conditions, the total deposition time was fixed at 30 minutes for all samples. The reactive gas pulsing process (RGPP) was implemented by varying the oxygen pulse duration (ton), while keeping the pulsing period (P = ton + toff) constant at 20 seconds. Accordingly, the toff values were set to 12 s, 8 s, and 0 s for ton values of 8 s, 12 s, and 20 s, respectively. This corresponds to duty cycles (α = ton / P) of 40%, 60%, and 100%. These conditions allowed systematic control of oxygen stoichiometry during the

deposition process and enabled a direct investigation of its influence on the physical and electrical properties of the SnO_x thin films. The effects of oxygen controlled pulsing process on the structural and surface morphology characteristics were studied via appropriate characterization techniques such as XRD and SEM imaging. The elemental compositions of the elaborated SnO_x thin-films via oxygen controlled pulsing process were extracted using energy-dispersive spectroscopy (EDS). In addition, the electrical properties of the elaborated SnO_x samples using RGPP method were extracted by carrying out Hall-effect measurements at room temperature. The idea behind the latter technique dwells in considering four metallic points aligned with the surface in contact with the prepared samples and then applying a current between two points and getting the associated voltage at the internal terminals. This technique enables estimating the film electrical parameters namely resistivity, carrier concentration, mobility and allows us to determine the conductive type of the prepared Snob thin-films.

2.2. SnOx TFT structure and analysis

To evaluate the impact of pulsed oxygen flow on the device performance, a calibrated TCAD simulation was performed using SILVACO software [22]. In this context, the electrical properties of the developed SnO_x thin-films with n-type and p-type conductivities are implemented in SILVACO software to analyze the performance of the SnO_x TFT device [22-23]. The electrical parameters (resistivity, mobility, carrier concentration) extracted from Hall Effect measurements were implemented into the TCAD model to reproduce the characteristics of SnO_x-based TFTs. Unlike conventional studies that simulate IGZO-based devices, our simulations are exclusively based on SnO_x I-V characteristics under various pulsing durations. In the model, a staggered bottom-gate TFT architecture was considered, and material parameters such as effective density of states, bandgap, and defect states were tailored based on experimental findings and literature values specific to SnO_x. For this purpose, we employed this software to solve the fundamental semiconductor equations namely the Poisson equation

and the continuity equations, using numerical differentiation and iteration method. These equations can be expressed as follows:

$$div(\varepsilon \nabla \psi) = -\rho \quad (1)$$

with $\rho = q(p - n + N_a)$

$$\frac{1}{q} div(\overrightarrow{J_n}) - R_n + G_n = 0 \quad (2)$$

$$-\frac{1}{q} div(\overrightarrow{J_p}) - R_p + G_p = 0 \quad (3)$$

where ε signifies the absolute permittivity, ψ represents the electrostatic potential. The net charge density, ρ is related to the P-type Si channel doping concentration (N_a) and the carrier densities of free electrons (n) and holes (p). Furthermore, J_n and J_p represent the current densities of electrons and holes, respectively. G_n and G_p denote the rates of generation, while R_n and R_p are the corresponding recombination rates.

Fig.1b shows its structure. The active layer is suggested with p-type and n-type SnO_x films. The latter can be elaborated using RGPP process, where tuning the oxygen concentration allows modulating the conductive behavior of SnO_x thin-film. A tree-terminal SnO_x TFT is considered using SiO_2 material as a gate oxide, where L is the channel length, d_{SnOx} and d_{SiO2} are respectively the channel and gate oxide thicknesses. The geometrical parameters of the analyzed SnO_x long-channel TFT devices are L=100 µm, d_{SnOx}=20 nm and d_{SiO2}=80 nm. To assess the accurateness of the developed model, the I_{ds}-V_{gs} characteristic of IGZO TFT obtained from the numerical investigation is compared and validated using experimental data provided in [24], as shown in Fig. 2. It can be seen that the developed numerical model can reproduce the experimental data, indicating the good accuracy of the model. It is important to note that the present work focused on a single TFT channel length to isolate the impact of the RGPP process on the intrinsic material properties of SnO_x. However, we acknowledge that device geometry significantly influences electrical performance parameters such as mobility, threshold voltage, and subthreshold swing. As a future direction, the proposed model can be extended by

investigating TFTs with varied channel lengths and widths to assess geometry-dependent behavior and validate the scalability and reproducibility of the approach. Additionally, complex phenomena such as short-channel effects, quantum confinement and tunnel effects should be taken into consideration.

The numerical model used in this work was calibrated using experimental data from IGZO-based TFTs, which exhibit similar amorphous oxide behavior and charge transport mechanisms. This benchmarking approach provides a solid foundation for simulating SnO_x TFT characteristics under varying oxygen conditions. However, due to current fabrication constraints, experimental characteristics of SnO_x-based TFTs are not yet available for direct validation. Future work will focus on fabricating and characterizing SnO_x TFT devices to directly compare simulated and measured data. This step is essential to further confirm the model's accuracy and establish its predictive power for optimizing SnO_x device architectures.

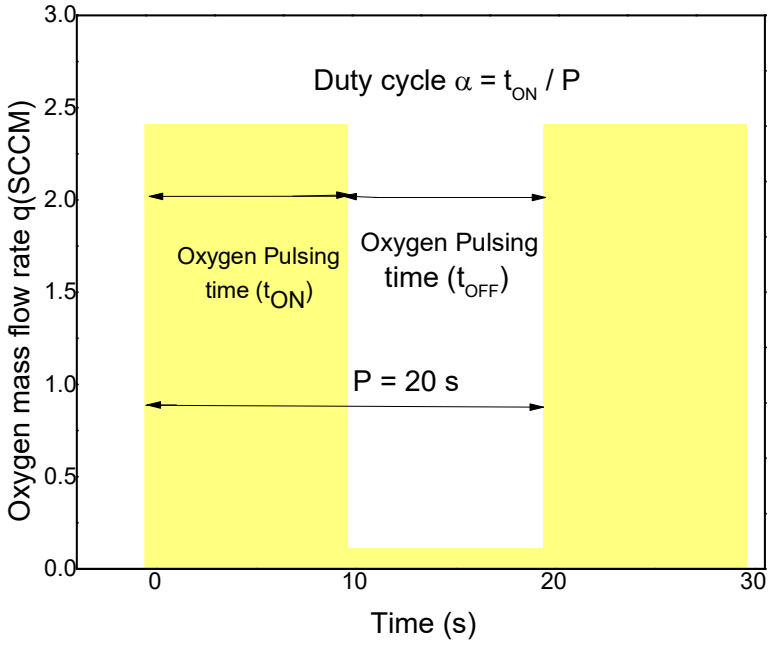

(a)

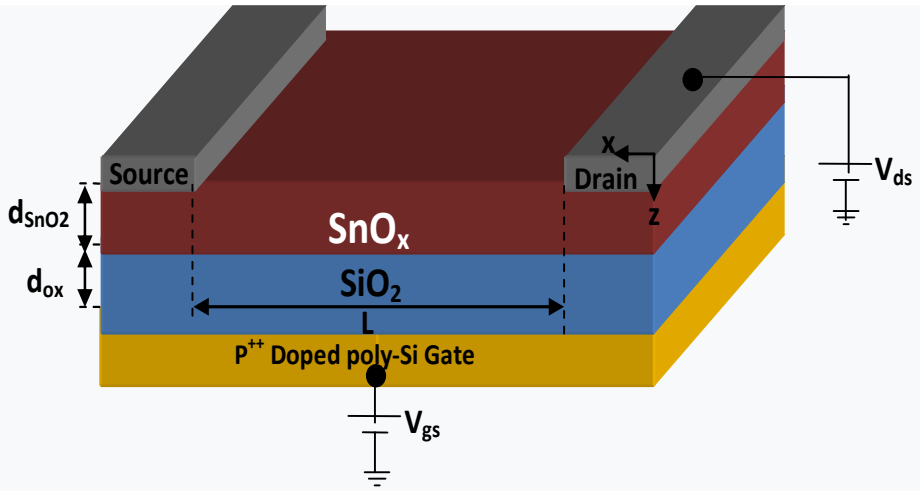

(b)

Figure.1: (a) Schematic description of RGPP process representing oxygen mass flow rate versus time **(b)** 3D-Schema of the investigated SnO_x thin-film transistor device.

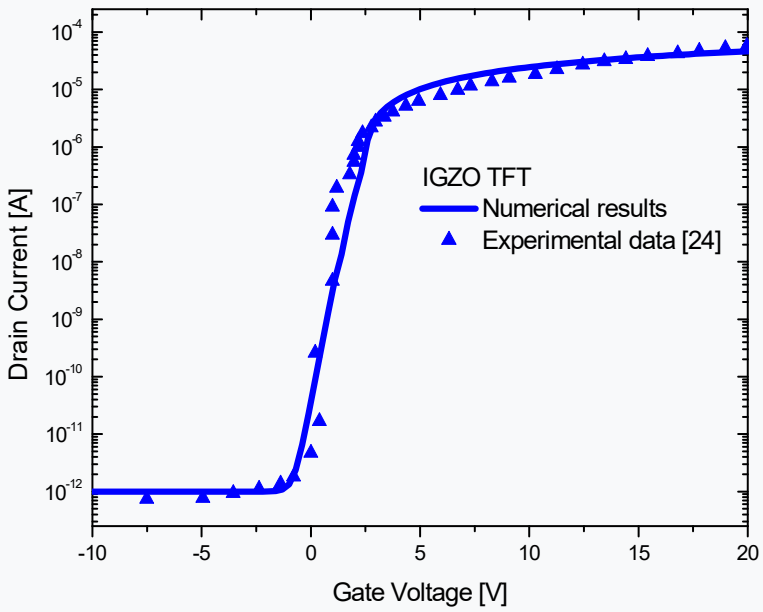

Figure.2: I_{ds}-V_{gs} characteristics of IGZO TFT numerical data and experimental ones.

3. Results and discussions

XRD measurements were performed for the elaborated samples to assess their structural properties. The obtained XRD patterns associated with the deposited SnO_x thin-films using various oxygen pulsing times in RGPP technique are shown in Fig. 3. The figure confirms that

the thin-film fabricated with t_{ON} = 0 s corresponds to the metallic growth mode of the RGPP technique, where the XRD pattern shows diffraction peaks of tetragonal tin material. In this deposition condition, we completely stopped the oxygen mass flow rate, thus leading to the sputtering of Sn metal at t_{ON} = 0 s [25]. On the other hand, the oxygen pulsing time increase leads to amorphous states for the elaborated SnO_x thin films, as proved by the absence of diffraction peaks in the corresponding XRD patterns. This is mainly due to the effect of oxygen, which disrupts the growth of crystalline phases in the SnO_x thin films. Furthermore, RGPP technique is basically related to the periodic injection of oxygen gas, which can in turn disturb the development of metal oxide material alloys on the target surface [25-26].

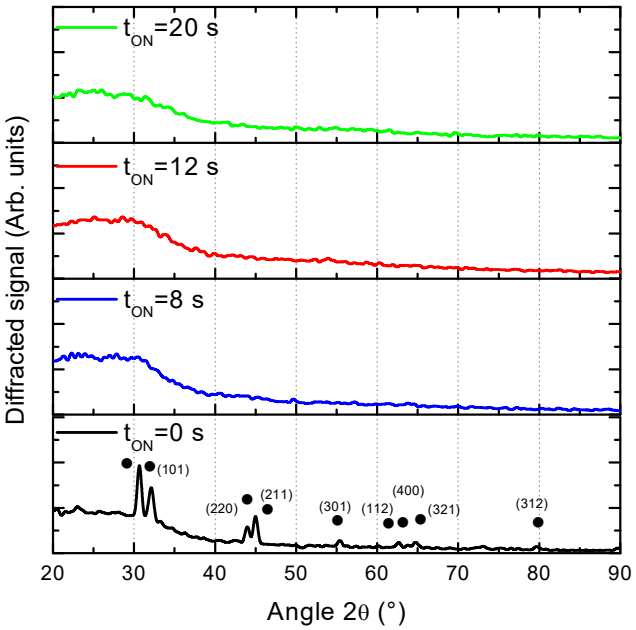

Figure.3: X-ray diffraction patterns of the prepared SnO_x samples using different t_{ON} times of 8 s, 12 s and 20 s during the RGPP.

The morphological characteristics of the SnO_x films, produced via combined RGPP and DC-sputtering growth methods, are investigated through performing SEM characterizations. Accordingly, Fig.4 presents high-magnification surface micrographs of the elaborated SnO_x thin films using RGPP process at dissimilar pulsing times of (a) t_{ON} =8 s , (b) t_{ON} =12 s and (c) t_{ON} = 20 s. On the other hand, Fig.4 (d) shows the cross-section SEM image of the prepared SnO_x thin-film at t_{ON} = 20 s. Fig. 4 (a), (b) and (c) show that granulated surface properties are obtained as the oxygen pulsing increases and the grains become more spherical and smaller with t_{ON} increase. In addition, the sample prepared at the oxidation growth mode shows a smoother surface. Extended ON-time results in a smoother and denser film, as depicted in Fig. 4 (c) and (d) at the same SEM magnification. Increasing the duty cycle (α > 80% of P) favors the oxidation sputtering mode [26], which reduces the deposition rate and stabilizes the oxygen concentration. The use of high duty cycle leads also to the formation of oxygen-rich SnO_x films, indicating that the oxidation sputtering mode is predominant under these elaboration conditions. Therefore, the sputtered Sn particles oxidize rapidly, forming Sn−O bonds and producing typical amorphous SnO_x thin films, as it is abovementioned (Fig. 3). Cross-sectional SEM image presented in Fig.4 (d) reveals that high oxygen pulsing time leads to the formation of homogeneous SnO_x thin-films. To support the claim that oxygen content in the SnO_x thin-films increases when high oxygen pulsing times are considered, an EDS analysis was performed to verify the presence of Sn and O elements in the sputtered Snob samples using RGPP method. The chemical compositions of the prepared thin-films are summarized in Table. 1. The EDS results closely agree with the SEM characterizations, showing that the oxygen level increases with rising the oxygen injection time. In this context, high oxygen concentration of 83 at.% is achieved for the prepared sample at t_{ON}=20 s, indicating the successful elaboration of oxygen-rich SnO_x thin-film. On the other hand, the tin concentration is found to be high as compared

to the oxygen level for low duty cycles. Importantly, no other elements were detected, signifying the high quality of the SnO_x thin-films.

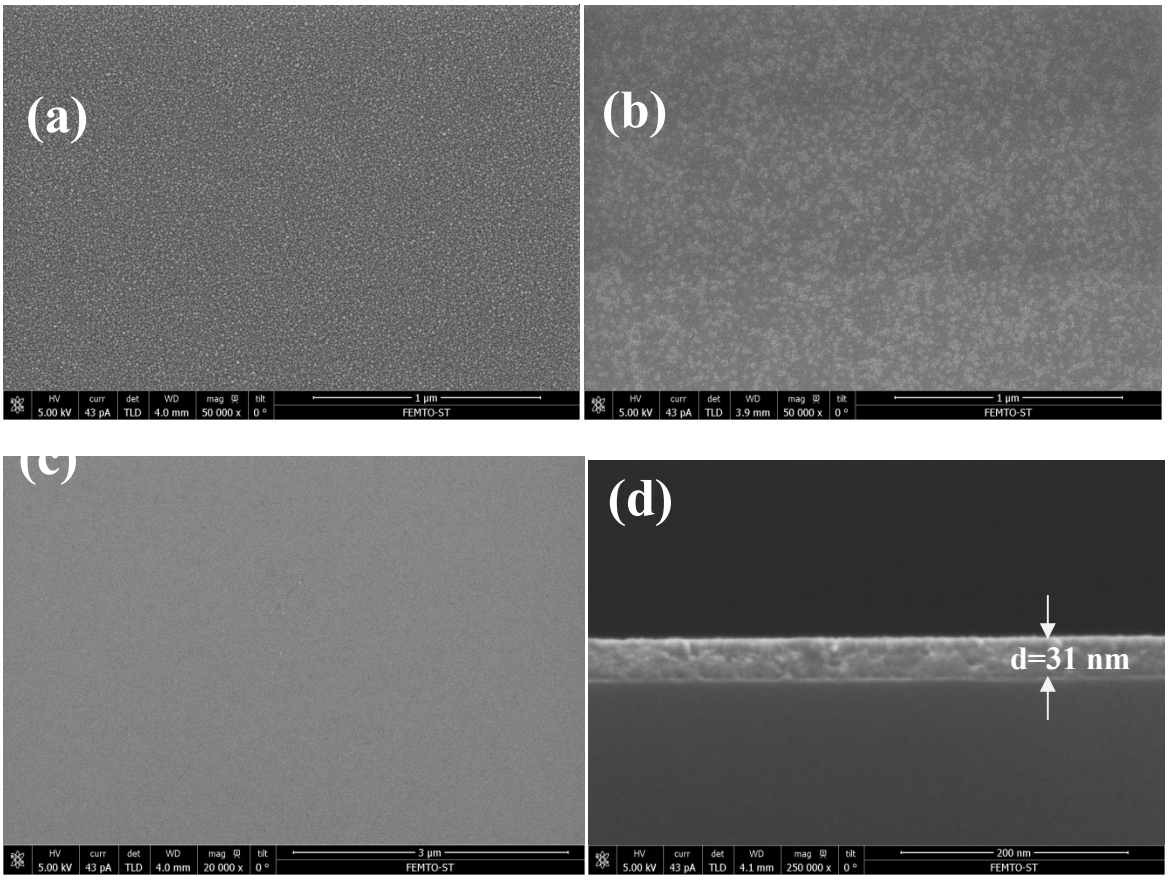

Figure.4: (a), **(b)** and **(c)** Top surface SEM images of SnO_x thin-layers deposited at various t_{ON} values of 8 s, 12 s and 20 s, respectively. **(d)** Cross-sectional micrograph of SnO_x thin-film fabricated using 20 s of oxygen injection time. for oxygen pulsing time of 8 s and with incident angles of **(c)** $\alpha = 0°$ and **(d)** $\alpha = 80°$. The same scale bar of 1 µm is used for the performed top surface SEM micrographs.

Table.1: Elemental composition extracted from *EDS* characterizations of the elaborated SnOx using different t_{ON} periods of 8 s, 12 s and 20 s during the RGPP technique.

Element	**Elaborated SnO_x thin-films at**		
	t=8 s	***t=12 s***	***t=20 s***
Sn	47.96 wt.%	22.53 wt.%	16.95 wt.%
O	52.04 wt.%	77.47 wt.%	83.05 wt.%

The evolution toward an amorphous structure in SnO_x films with increasing t_{ON} is closely related to the enhanced oxygen content, as evidenced by EDS analysis. Higher oxygen

incorporation can lead to the formation of non-stoichiometric defects and increased disorder within the Sn–O bonding network, thus disrupting crystallinity. This phenomenon has also been observed in other oxide systems under oxygen-rich conditions [27]. While SEM images qualitatively suggest grain refinement and improved film uniformity with increasing *ton*, we acknowledge that the absence of quantitative grain size analysis and surface roughness measurements limits a more rigorous assessment. Due to current experimental constraints, such characterizations could not be performed in this study. However, these aspects will be addressed in future work to further validate the trends observed and to provide a more comprehensive understanding of the structural evolution of SnO_x thin films under reactive gas pulsing conditions.

To gain a deep insight regarding the electronic characteristics of the developed SnOx thin-films at various oxygen injection periods, the band gap (Eg) of the prepared samples is extracted from Tauc plots provided in Fig.5. Observing this figure, Eg increases with t_{ON} increase, reaching a maximum of approximately Eg=3.59 eV, which correlates with the band gap value of SnO_2 compound [27]. On the other hand, the prepared thin-film using t_{ON}=8 s shows lower band gap value of 2.56 eV. The latter value is very close to that found in recently published works [28-30]. The increase in the band gap is attributed to the higher oxygen content in the SnO_x thin-film as confirmed by the EDS measurements. This reduces the density of oxygen vacancies in the over-stoichiometric SnO_2 film, leading to the band gap increase.

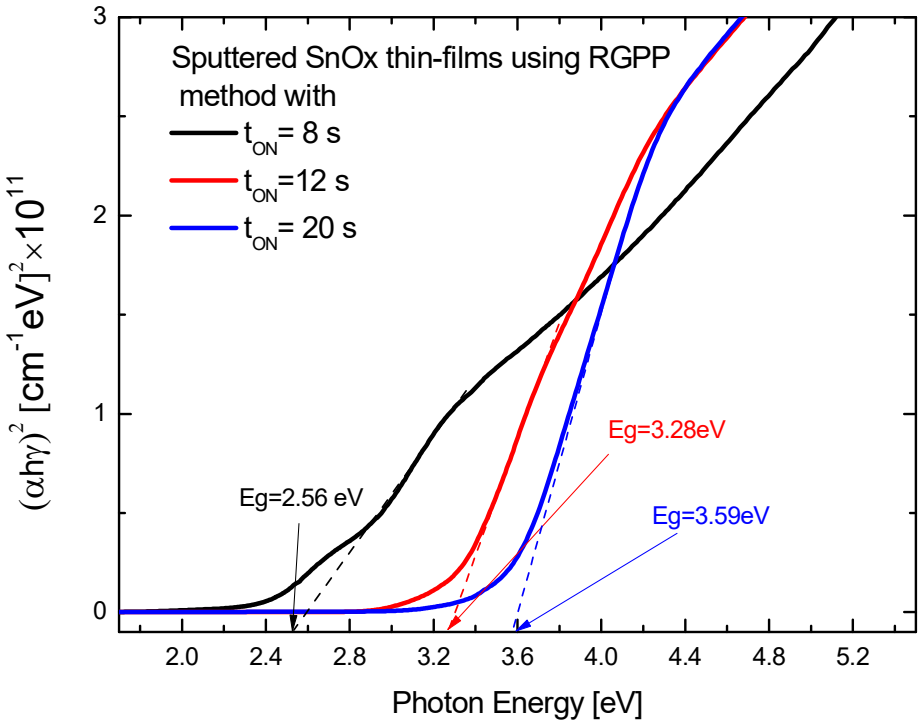

Figure.5: Tauc plots of the elaborated tin oxide thin-layers using different t_{ON} values of 8 s, 12 s and 20 s.

In order to investigate the electrical properties of the prepared SnO_x thin-films using dissimilar pulsing times of RGPP method, Hall measurements were carried out for the elaborated SnO_x-based samples at dissimilar oxygen injection periods. In this framework, the variation in electrical performance of SnO_x TFTs with respect to oxygen pulsing duration can be attributed to the modulation of oxygen vacancy concentration and its impact on carrier transport. Shorter pulsing durations (e.g., 8 s) result in relatively oxygen-deficient films, leading to an abundance of oxygen vacancies that act as shallow donors, thereby enhancing n-type conductivity. Conversely, longer pulsing durations (e.g., 20 s) favor oxygen-rich conditions, reducing vacancy concentration and promoting the formation of acceptor-like defects, which can suppress electron mobility or induce p-type behavior. At the optimal pulsing duration of 12 s, a balanced oxygen stoichiometry is achieved, minimizing both excessive donor or acceptor

defects and enhancing the crystalline quality and carrier mobility. This explains the superior ON current and ON/OFF current ratio observed under this condition. These trends are further supported by band alignment analysis and Hall measurement data, which confirm the strong correlation between reactive gas modulation, defect states, and device-level electrical performance. Moreover, the associated electrical parameters at room temperature namely electrical conductivity, carrier concentration, carrier mobility and conductive type of the elaborated thin-films are summarized in Table. 2. It can be demonstrated from this table that the elaborated SnO_x film at 8 s of pulsing time shows p-type semiconducting behavior with a high carrier mobility of 12 $cm^2/V.s$. On the other hand, the elaborated sample using a pulsing time of t_{ON} = 12 s exhibits n-type conductivity with a favorable carrier mobility of 11 $cm^2/V.s$, low resistivity of 8.5 Ω.cm and carrier concentration of 1.2×10^{16} cm^{-3}. This indicates the ability of combined RGPP and DC sputtering technique for the elaboration of high electrical performance SnO_x thin-films with tunable semiconducting conductive type. This behavior is mainly correlated with the variation of the oxygen concentration in the film when RGPP with controllable oxygen injection time is considered. In other words, long pulsing time leads to increase the oxygen level in the film, allowing the formation of n-type semiconductor. Therefore, the obtained conductive behavior of the prepared SnO_x films indicates their potential use as active layers in n-TFT and p-TFT devices. For this reason, the electrical parameters of the fabricated SnO_x thin-films using RGPP process are implemented in SnOx TFT devices and then analyzed. In this context, Fig.6 shows Ids-Vgs characteristics associated with the investigated TFT devices based on SnO_x active layers realized at 8 s and 12 s oxygen injection times compared to that of the conventional TFT device. This figure shows that the analyzed SnO_x-based devices show an enhanced derived current as compared to traditional TFT device. This is mainly related to the high carrier mobility offered by the elaborated SnOx thin-films using combined RGPP and DC sputtering techniques. The proposed TFT device based on n-

type SnOx elaborated using RGPP shows a threshold voltage shift to positive voltages. This shift can be attributed to the high carrier concentration associated with the developed film at 12 s of pulsing time. In addition, a low off-state current is achieved due to the good resistive behavior of the prepared films with varied oxygen content. The investigated p-SnO_x TFT device exhibits a very low off-state current and high ON current, indicating its high electrical performances as compared to the conventional device.

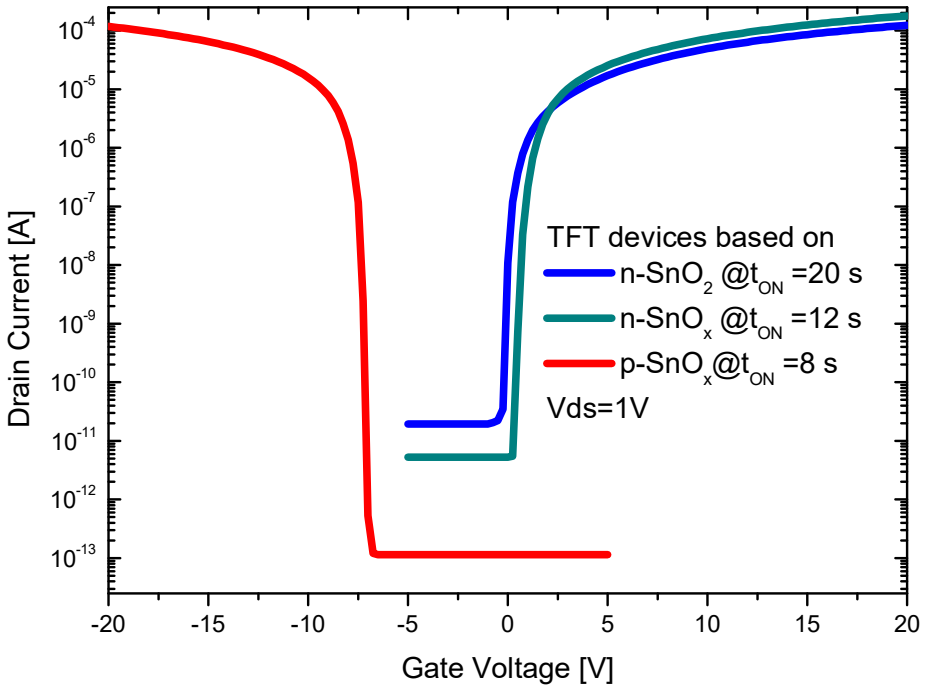

Figure.6: I_{ds}-V_{gs} characteristics of the proposed TFT devices based on n-type and p-type SnO_x compared to the conventional SnO_2-based device.

Table.2: Electrical properties of the DC-sputtered SnO_x thin-films.

Electrical properties	**SnOx thin-films elaborated at the oxygen injection time of**		
	t=8 s	***t=12 s***	***t=20 s***
Resistivity [Ω.cm]	10, 7	8.5	4.5
Carrier Concentration [cm^{-3}]	2.1×10^{16}	1.2×10^{16}	2.5×10^{16}
Carrier Mobility [$cm^2/V.s$]	11.7	11	3.4
Conduction type	p-type	n-type	n-type

The transition from p-type to n-type conductivity observed in the Hall Effect measurements can be directly linked to the variation in oxygen stoichiometry induced by the reactive gas pulsing process. Under oxygen-rich conditions (short t_{ON}), the formation of acceptor-like defects such as tin vacancies and interstitial oxygen is favored, which introduces holes and results in p-type conductivity. As t_{ON} increases, the oxygen incorporation becomes more significant, eventually saturating the available defect sites and reducing the concentration of acceptor states. Simultaneously, oxygen vacancies, which act as shallow donor states, begin to dominate, thus shifting the conductivity to n-type. This transition is also reflected in the observed changes in carrier mobility and resistivity. The increase in carrier concentration associated with donor-like defects improves conductivity, while the disorder introduced by excessive oxygen may scatter carriers, affecting mobility. The combined influence of these competing factors determines the overall electrical behavior of the SnO_x films and highlights the critical role of oxygen stoichiometry in tuning their electronic properties.

To further assess the electrical performance of the proposed TFT devices based on SnO_x thin-layers with p-type and n-type conduction properties, Table.3 recapitulates the electrical performances of the proposed TFT devices based on the prepared p-type and n-type SnO_x thin-films compared with that of recently published works using various metal oxide material building blocks [31-39]. It can be demonstrated from this table that the proposed TFT devices based on SnO_x thin-films elaborated using RGPP method outperforms greatly the other n-TFT devices in terms of electrical performances, offering a high ON-to-OFF current ratio of 207 dB and a low OFF state current of 5×10^{-4} nA. In addition, the elaborated p-type SnO_x thin-film provides the possibility for designing high performance TFT device, showing a superior I_{ON}/I_{OFF} ratio of 220 dB and a low noise current of 1.1×10^{-4} nA. The obtained electrical performances are higher than that of conventional p-TFT devices based on various p-type metal oxide materials. Therefore, we believed that the use of combined RGPP and DC sputtering

technique could open up new pathways for the elaboration of high-performance TFT devices with tunable conduction type, which are highly suitable for flexible electronic applications. It is worth noting that the comparative analysis between the proposed SnO_x TFTs and other reported metal oxide-based TFTs highlights general performance trends. However, certain key parameters, such as the subthreshold swing (SS), are not reported in some of the referenced studies. These entries have been marked as "N/A" (Not Available) in the table to ensure transparency. Despite this limitation, the available data allow for a meaningful evaluation of device behavior, particularly regarding OFF-current and ON/OFF current ratio. While the present investigation has successfully demonstrated the influence of the reactive gas pulsing process (RGPP) on the structural and electrical performance of SnO_x-based TFTs, further studies are needed to assess the long-term stability and reliability of the proposed devices. In this context, advanced reliability tests such as Negative Bias Temperature Instability (NBTI) and Positive Bias Temperature Stress (PBTS) are highly recommended [40]. These tests are essential to evaluate threshold voltage stability and charge trapping phenomena under prolonged gate bias stress conditions, which are critical for practical applications in wearable and flexible electronics. Future work will focus on implementing these reliability protocols to monitor performance degradation over time and to identify possible failure mechanisms. In addition, it would be beneficial to perform comprehensive band alignment studies using experimental techniques or simulation tools to better understand the role of oxygen modulation via RGPP on the electronic conduction mechanism and energy level distribution at the interfaces. Overall, integrating reliability assessments and electronic structure analysis will significantly strengthen the applicability of SnOx-based TFTs and contribute to the development of cost-effective and robust oxide-based electronic devices free from critical raw materials.

Table.3: Electrical performance comparison between the proposed SnO_x-based TFTs and other device structures based on various metal oxide materials.

TFT device structures	Electrical performance parameters			Ref.
	I_{ON}/I_{OFF} (dB)	I_{OFF} (nA)	Swing factor (mV/dec)	
In-doped SnO thin-film	123.5	9×10^{-3}	400	[31]
CuGaO thin film	80.2	N/A	519	[32]
SnGaO thin-film	81.8	9×10^{-3}	550	[33]
InGaSnO thin film	173	N/A	210	[34]
$SnS_{0.2}O_{0.8}$ thin-film	68.6	2.9×10^{-2}	N/A	[35]
SnO_2 channel/Al_2O_3 dielectric gate	128.3	N/A	260	[36]
Zr-SnO_xchannel/ZrO_2 dielectric gate	133.8	8×10^{-3}	191	[37]
SnO thin-film	85	7×10^{-1}	N/A	[38]
SnO channel	90	9×10^{-2}	N/A	[39]
SnO_2-based TFT @ t_{ON} = 20 s	151	5.2×10^{-3}	161.5	This work
SnO_x-based TFT @ t_{ON} = 12 s	136.2	1.9×10^{-2}	143.1	This work
SnO_x-based TFT @ t_{ON} = 8 s	176.4	1.2×10^{-4}	124.3	This work

4. Conclusion

This paper investigates the role of combined oxygen controlled pulsing process and DC sputtering for the elaboration of SnO_x thin-films with tunable electrical properties. The latter can be achieved by considering varied oxygen injection times in the RGPP technique. Hall measurements were performed to assess the electrical performances of the prepared samples where the resistivity, carrier mobility and concentration parameters were extracted. It is revealed that the SnO_x electrical characteristics can be tuned by using RGPP technique, enabling the variation of the oxygen concentration in the film. The experimentally extracted electrical parameters of p-type and n-type SnO_x thin-films were implimented to investigate the performance of the corresponding TFT devices using an accurate numerical modeling approach.

It is demonstrated that the invetigated devices exhibit high derived current, while maintaining low off-state current, where an ON-to-OFF current ratio of 176.4 dB is recorded . This improvement can be attributed to the high carrier mobility of 11.7 cm^2/V.s. Therefore, we believe that the present study can open up new pathways for the fabrication of cost-effective SnO_x thin-films with tunable electrical properties, which can be approriate for thin-film electronic applications. Although the proposed SnO_x TFTs exhibit promising electrical characteristics under initial measurement conditions, a comprehensive evaluation of their stability under electrical and environmental stress remains essential for practical applications. Due to current equipment and device fabrication constraints, short-term bias stress measurements (e.g., under positive/negative gate bias for several hours) and environmental stability tests (e.g., exposure to humidity and temperature cycling) could not be conducted in this study. These assessments are planned as part of future work and will include long-term stress protocols such as Negative Bias Temperature Instability (NBTI) and Positive Bias Temperature Stress (PBTS). Such investigations will provide deeper insights into the reliability and suitability of SnO_x-based TFTs for integration into flexible and wearable electronic platforms.

Data Availability

The data utilized in this study is proprietary to the authors and will not be publicly shared.

Funding

There is no funding.

Authors and Affiliations

LEA, Department of Electronics, University of Batna 2, Algeria.
F. Djeffal and H. Ferhati
ISTA, University of Larbi Ben M'hidi, Oum El Bouaghi, Algeria.
H. Ferhati

SUPMICROTECH, CNRS, Institut FEMTO-ST, 15B, Avenue des montboucons 25030 BESANCON Cedex, France.

N. Martin

Contributions

F. Djeffal and H. Ferhati contributed to conceptualization, formal analysis, drafting the manuscript. N. Martin and F. Djeffal contributed to formal analysis, revising the manuscript critically for important intellectual content.

Ethics declarations

Competing interests

The authors declare that they have no competing interests.

Ethics approval and consent to participate

Not applicable.

Consent for publication

Not applicable.

References

[1] K. Shrivas, at. al, "Advances in flexible electronics and electrochemical sensors using conducting nanomaterials: A review," Microchemical Journal, vol.156, pp. 104944, 2020.

[2] T. Pan, S. Liu, L. Zhang, W. Xie, "Flexible organic optoelectronic devices on paper," iScience, vol.25, pp. 103782, 2022.

[3] Z. Wang and G. Shen, "Flexible optoelectronic sensors: status and prospects," Mater. Chem. Front., vol.7, pp. 1496-1519, 2023.

[4] A. Azarov, A. Hallén, H.H. Radamson, "Electrical Characterization of Semiconductors: I–V, C–V and Hall Measurements," In: Analytical Methods and Instruments for Micro- and Nanomaterials. Lecture Notes in Nanoscale Science and Technology, vol 23, pp.197-240, 2023, Springer, Cham. https://doi.org/10.1007/978-3-031-26434-4_7.

[5] H. Ferhati and F. Djeffal, "Giant responsivity of a new InGaZnO ultraviolet thin-film phototransistor based on combined dual gate engineering and surface decorated Ag nanoparticles aspects," Sensors and Actuators A: Physical, vol. 318, pp. 112523, 2021.

[6] H. Ferhati, F. Djeffal, L.B. Drissi, "Performance analysis of a new Mid-Infrared phototransistor based on combined graded band gap GeSn sensitive-film and IGZO TFT platform," Micro and Nanostructures, vol.173, pp. 207467, 2023.

[7] M. Akbari-Saatlu et al., “Ultrasensitive H2S and CH3SH Sensors Based on SnO2 Porous Structures Utilizing Combination of Flame and Ultrasonic Spray Pyrolysis Methods,” IEEE Sensors Journal, vol. 24, pp. 36393-36402, 2024, doi: 10.1109/JSEN.2024.3467168.

[8] M. Akbari-Saatlu, et al., “Nanometer-thick ZnO/SnO2 heterostructures grown on alumina for H2S sensing,” ACS Applied Nano Materials, vol. 5, pp. 6954-6963, 2022.

[9] Y. Ma, et al., “First-principles-based quantum transport simulations of high-performance and low-power MOSFETs based on monolayer Ga2O3,” ACS Applied Materials & Interfaces, vol. 14, pp. 48220-48228, 2022.

[10] K. Kandpal, et al, “Study of ZnO/BST interface for thin-film transistor (TFT) applications,” Surfaces and Interfaces, vol. 23, pp. 100996, 2021.

[11] X. Liu, et al, “Transparent, High-Performance Thin-Film Transistors with an InGaZnO/Aligned-SnO2-Nanowire Composite and their Application in Photodetectors,” Advanced Materials, vol. 26, pp. 7399–7404, 2014.

[12] F. Shan, et al, “High-mobility p-type NiOx thin-film transistors processed at low temperatures with Al2O3 high-k dielectric,” J. Mater. Chem. C, vol. 4, pp. 9438-9444, 2016.

[13] J. Yu, et al, “Solution-processed p-type copper oxide thin-film transistors fabricated by using a one-step vacuum annealing technique,” J. Mater. Chem. C, vol. 3, pp. 9509-9513, 2015.

[14] L. Lei, et al, “Low-voltage solution-processed Cuprous thiocyanate Thin-Film transistors with NAND logic function,” Results in Physics, vol. 3, pp. 106764, 2023.

[15] R. Djamil, K. Aicha, A. Souifi, F. Djeffal, “Effect of annealing time on the performance of tin oxide thin films ultraviolet photodetectors,” Thin Solid Films, vol. 623, pp. 1-7, 2017.

[16] F. Djeffal, N. Martin and H. Ferhati, “Tunable band-selective photodetector based on sputter-deposited SnOx thin-films: Effect of reactive gas pulsing process,” Journal of Alloys and Compounds, vol. 968, pp. 171851, 2023.

[17] A. K. Gangwa, et al, “Temperature-dependent p-n switching for highly selective CO gas sensing based on mixed phases of magnetron sputtered (p)SnO-(n)SnO2 thin films,” Applied Surface Science, vol. 655, pp. 159607, 2023.

[18] H. Ferhati et al. “Tunable properties of SnO_x sputter-deposited by RGPP and GLAD techniques: A potential candidate for photosensing and all-oxide solar cells,” Solar Energy, vol.268, pp. 112305, 2024.

[19] E. Aubry, S. Weber, A. Billard, N. Martin, “Enhanced tunability of the composition in silicon oxynitride thin films by the reactive gas pulsing process”, Appl. Surf. Sci., vol. 290, pp. 148-153, 2014.

[20] M. Grafouté, C. Petitjean, A. Diama, J. F. Pierson, J. M. Greneche, C. Rousselot, “Structural investigations of iron oxynitride multilayered films obtained by reactive gas pulsing process,” Surf. Coat. Technol., vol. 272, pp. 158-164, 2015.

[21] X. Xu, M. A. P. Yazdi, R. Salut, J-M. Cote, A. Billard, N. Martin, “Structure, composition and electronic transport properties of tungsten oxide thin film sputter-deposited by the reactive gas pulsing process,” Mater. Chem. Phys., vol. 205, pp. 391-400, 2018.

[22] K. Kacha, et al., “Numerical investigation of a double-junction a: SiGe thin-film solar cell including the multi-trench region,” Journal of Semiconductors, vol. 36, pp. 064004, 2015.

[23] Atlas User’s manual, SILVACO TCAD, 2019.

[24] Yen-Lin Chu, et al., “Fabrication and Characterization of a-IGZO Thin-Film Transistors With and Without Passivation Layers,” ECS J. Solid State Sci. Technol, vol. 10, pp. 027002, 2021.

[25] A. Cacucci, V. Potin, L. Imhoff, N. Martin, “Structural and electrical properties in tungsten/tungsten oxide multilayers”, Thin Solid Films, vol. 553, pp. 93-97, 2014.

[26] N. Parreira, T. Polcar, A. Cavaleiro, “Characterization of W-O coatings deposited by magnetron sputtering with reactive gas pulsing”, Surf. Coat. Technol., vol.201, pp. 5481-5486, 2007.

[27] H.H. Radamson, et al., “CMOS scaling for the 5 nm node and beyond: Device, process and technology,” Nanomaterials, vol. 14, pp. 837, 2024.

[28] K. Javaid, et al. “Structural and thermoelectric properties of nanostructured p-SnO thin films grown by e-beam evaporation method”, International Journal of Hydrogen Energy, vol. 47, pp. 15547-15555, 2022.

[29] C. K. G. Kwo, et al. “ Conversion of p-type SnO to n-type SnO2 via oxidation and the band offset and rectification of an all-Tin oxide p-n junction structure”, Applied Surface Science, vol. 627, pp. 157295, 2023.

[30] M. A. Alnuwaiser, et al. “Annealing induced morphology evolution and phase transition in SnOx thin films grown by e-beam evaporation method”, Inorganic Chemistry Communications, vol. 140, pp. 109473, 2022.

[31] Y-F. Wei, T. Zhang, J-J. Wu, T-J. Li, D. Lin, “Mobility enhancement of tin oxide thin-film transistor by indium-doping,” Vacuum, vol. 221, pp. 112868, 2024.

[32] A. Singh, G. R. Perumallapelli, R. N. Bukke, “High-performance of low temperature solution-processed P-channel CuGaO thin film transistors,” Journal of Alloys and Compounds, vol. 996, pp. 174801, 2024.

[33] Y. Lu, X. Dai, J. Yang, Y. Liu , D. Cao, F. Lin , F. Liu “Enhancement of electrical characteristics of SnGaO thin-film transistors via argon and oxygen plasma treatment,” Vacuum, vol. 225, pp. 113208, 2024.

[34] Z. Song, M. Hu , X. Zhang , Z. Zhu , S. Luo , L. X, “High mobility and hysteresis free InGaSnO thin film transistors by co-sputtering via low temperature post annealing process,” Thin Solid Films, vol. 795, pp. 140309, 2024.

[35] T. Zhang, W. Wang, Y. Liu, F. Wang, X. Pan, B Lu, Z. Ye, “Influence of post-deposition annealing on the novel alloyed SnSxO1-x semiconductor in p-type thin-film transistors,” Materials Science in Semiconductor Processing, vol. 151, pp. 107037, 2022.

[36] Y-F. Wei, T. Zhang, J-J. Wu, T-J. Li, D. Lin, “High-Mobility Solution-Processed Tin Oxide Thin-Film Transistors with High-κ Alumina Dielectric Working in Enhancement Mode,” ACS Applied Materials & Interfaces, vol. 6, pp. 20786–20794, 2014.

[37] Z. Wang et al., “Doping Effects of Various Carrier Suppressing Elements on Solution-Processed SnOx-Based Thin-Film Transistors,” IEEE Transactions on Electron Devices, vol. 66, pp. 3371-3375, 2019.

[38] M. G. Chae, S. H. Han, B. K. Park, T-M. Chung, J. H. Han, “Atomic-layer-deposited SnO film using novel Sn(dmamb)2 precursor for p-channel thin film transistor,” Applied Surface Science, vol. 547, pp. 148758, 2021.

[39] M. P. Hung, et al, “Off-current reduction in p-type SnO thin film transistors,” Appl. Phys. Lett., vol.112, pp. 263502, 2018.

[40] F. Djeffal, S. Guessasma, A. Benhaya, M. Chahdi, “An analytical approach based on neural computation to estimate the lifetime of deep submicron MOSFETs,” Semiconductor science and technology, vol. 20, pp. 158, 2005.